JOURNAL OF COMPUTATIONAL PHYSICS 105, 122–132 (1993)

# Numerical Chaos, Symplectic Integrators, and Exponentially Small Splitting Distances

B. M. HERBST

*Department of Applied Mathematics, University of the Orange Free State, Bloemfontein 9300, South Africa*

AND

MARK J. ABLOWITZ

*Program in Applied Mathematics, University of Colorado, Boulder, Colorado 80309-0526*

Received June 17, 1991; revised May 14, 1992

Two discrete versions of Duffing's equation are derived as reductions of discretizations of the nonlinear Schrödinger (NLS) equation. Inheriting the properties of the NSL discretizations, one is shown to be integrable and, using a Mel'nikov type analysis, the other discretization is shown to be nonintegrable. Arguments are given why it is possible for the nonintegrable scheme to restore the homoclinic orbit at an exponentially fast rate which is faster than the order of the approximation, as $h \to 0$. This suggests why there can be fundamental differences between symplectic and nonsymplectic discretizations of certain continuous Hamiltonian systems. 

## 1. INTRODUCTION

In finite-dimensional nonlinear dynamical systems it is well known that underlying homoclinic structures act as the source of chaos under small perturbations of the system. More recently, homoclinic structures have also been discovered in the integrable equations of soliton theory. The effects of small perturbations, in the form of small forcing and damping terms, added to the integrable system have been studied in detail, see, for example, [1–3] and from these studies it has become clear that the homoclinic structures can act as sources of chaos in infinite-dimensional systems. In finite-dimensional systems a standard way of establishing that the conditions for chaos are met is through a Mel'nikov type analysis. Such an analysis has been applied to a certain finite-dimensional projection of the infinite dimensional damped-driven nonlinear Schroedinger (NLS) equation [4].

Our own interest has been in the consequences of the presence of homoclinic structures for numerical discretizations; in particular, those that still maintain the Hamiltonian nature of the problem, see [6–9]. As an illustration, consider the NLS equation,

$$iq_t + q_{xx} + 2|q|^2 q = 0, \tag{1}$$

with periodic boundary conditions, $q(x, t) = q(x + L, t)$. The NLS equation has many features that are familiar from finite dimensional systems. For instance, there is a natural way to view it as a completely integrable Hamiltonian system, see, for example, [10]. The focusing equation has also been recognized to possess a denumerable infinity of homoclinic/heteroclinic orbits in time. Contrary to what one might normally expect in infinite dimensions, the homoclinic orbits under certain conditions divide infinite-dimensional phase space in a very specific and natural way, see, for example, [3, 9] (an earlier reference giving the expression for the single homoclinic orbit is [5]). Note that, since the NLS equation is completely integrable, no stochasticity or chaos is associated with it.

Let us now investigate what happens if we solve the NLS equation numerically, choosing initial conditions in the vicinity of a homoclinic/heteroclinic orbit. The standard second-order finite difference replacement of (1) is given by

$$i\dot{Q}_n + (Q_{n-1} - 2Q_n + Q_{n+1})/h^2 + 2|Q_n|^2 Q_n = 0. \tag{2}$$

In addition, we use $L = 4\sqrt{2}\pi$, $N = 32$, where $h = L/N$ and an initial condition of the form,

$$q(x, 0) = a(1 + \varepsilon_1 \alpha_1 \cos(\mu x) + \varepsilon_2 \alpha_2 \cos(2\mu x)),$$

where $|\varepsilon_1|, |\varepsilon_2| \ll 1$, $\mu = 2\pi/L$, and $\alpha_1$, $\alpha_2$ are complex constants. The solution shown in Fig. 1 is obtained by choosing $\alpha_1$, $\alpha_2$ such that the initial condition is aligned in the direc-

0021-9991/93 $5.00

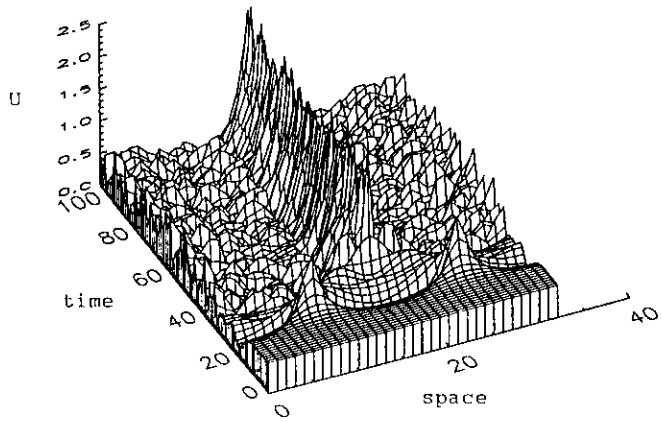


**FIG. 1.** The solution of the standard discretization (2).

tion of the double homoclinic orbit, see [8]. The solution is clearly irregular, even chaotic, unlike the analytical solutions of the NLS equation. The main mechanism driving this instability has been traced to a breakup of the homoclinic orbit under the discretization, allowing frequent homoclinic crossings—a main source for chaos in finite-dimensional systems. Since the method is convergent we find that all irregularities disappear as they should as $h \to 0$.

The discretization of the nonlinear term is now changed to

$$i\dot{Q}_n + (Q_{n-1} - 2Q_n + Q_{n+1})/h^2 + |Q_n|^2 (Q_{n-1} + Q_{n+1}) = 0, \tag{3}$$

which is still of second-order accuracy. The numerical solution obtained from this discretization displays no irregularities as shown in Fig. 2, using the same parameter values as in Fig. 1. This is the qualitative behavior one would expect from a completely integrable equation. The reason for the superior performance of the second method, (3), is that it has been carefully designed to be *integrable* [16]. Integrability, in the context of this discussion, means that the homoclinic structure is preserved. The integrable discretization does not allow homoclinic crossings and no chaotic behavior has been observed.

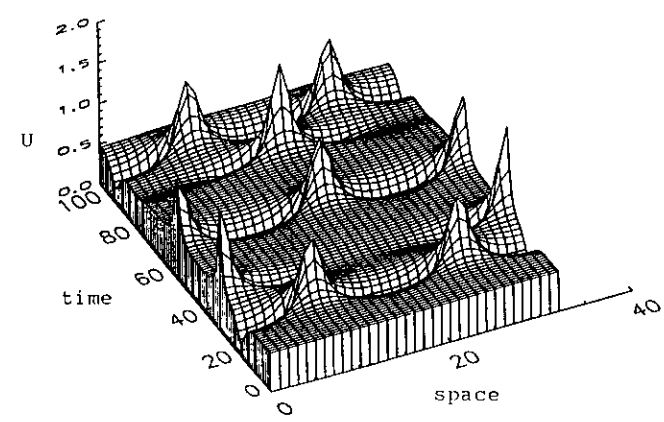


**FIG. 2.** The solution of the integrable discretization (3).

The proposition that homoclinic crossings are responsible for the instabilities associated with the nonintegrable discretization (2), receives further support from the study of McLaughlin and Schober [11]. Their numerical nonlinear mode analysis shows that frequent homoclinic crossings are associated with the numerical discrepancies.

In this paper we follow a different approach. A reduction of the NLS equation leads to Duffing's equation. Employing similar reductions to the discretizations (2) and (3), we arrive at integrable and nonintegrable discretizations of Duffing's equation (other discretizations could also be considered). In the case of the integrable discretization we show that the constants of motion as well as the expression for the homoclinic orbit follow from *systematically* applying the reduction to the integrable scheme (3). We note that this procedure is quite general—and algorithmic—and is useful to derive integrable discretizations in higher dimensions as well, see [12]. Having obtained an integrable discretization of Duffing's equation, the main idea (see (6) and (19)) is to view the nonintegrable discretization as a perturbation of the integrable discretization. We note also [13] which studies particular linear perturbations of the integrable discretization (19) and they are able to evaluate the Mel'nikov function in closed form. We, on the other hand, are interested in perturbations introduced by discretizing the equations for numerical purposes. The Mel'nikov analysis is performed in order to determine how the splitting distance, between the perturbed stable and unstable manifolds, behaves as a function of $h$. We find it convenient to consider a family of perturbations which are more amenable to a Mel'nikov-type analysis. This enables us to establish that the chaos in the nonintegrable discretization is indeed due to frequent homoclinic crossings. In addition, the analysis suggests that the chaotic region around the unperturbed homoclinic orbit will become exponentially small as $h \to 0$. This is in sharp contrast to the accuracy of the discretization which remains second order. Reasons are given as to why this desirable feature is intimately connected with the symplectic (area preserving) nature of the discretization. We argue that our observation in connection with Duffing's equation is generic and sheds light on the behavior of general symplectic discretizations of planar (integrable) Hamiltonian systems. In order to find additional justification for this claim, numerical experiments are performed with the second- and fourth-order symplectic schemes of Ruth and Forest [14]. These experiments also indicate that there is apparently little difference from a qualitative point of view, between lower and higher order symplectic methods.

## 2. DUFFING'S EQUATION AS A REDUCTION OF THE NLS EQUATION

Assume a solution of (1) of the form $q(x,t) = \exp(i\omega t)\, u(x)$, where $u(x)$ is a real function and $\omega$ is a real parameter. Without loss of generality we can take $\omega = 1$. It follows that $u(x)$ satisfies Duffing's equation in the form

$$u_{xx} - u + 2u^3 = 0. \tag{4}$$

Applying a similar reduction to the integrable discretization (3), we obtain the map,

$$\begin{aligned} &U_{n+1} - 2U_n + U_{n-1} - h^2 U_n \\ &\quad + h^2 U_n^2 (U_{n-1} + U_{n+1}) = 0, \end{aligned} \tag{5}$$

which can be rewritten as a system of first-order equations,

$$\begin{aligned} U_{n+1} &= V_n \\ V_{n+1} &= -U_n + \frac{2\mu V_n}{1 + h^2 V_n^2}, \end{aligned} \tag{6}$$

where $\mu = 1 + \frac{1}{2}h^2$.

It is not immediately clear that this map inherits the integrable properties of the original integrable discretization (3). Although one may recognize it as belonging to the family studied by McMillan [15], we note that its integrability follows systematically from a reduction of (3). For this purpose we find the conservation law associated with (3). It is obtained using techniques similar to those of Ablowitz and Ladik [16] to obtain the constants of motion for the integrable discretization (3). In order to make this paper self-contained we describe the procedure briefly.

The integrable discretizations of the equations in the NLS hierarchy derive from the compatibility condition between

$$\begin{aligned} \phi_{1_{n+1}} &= z\phi_{1_n} + hQ_n\phi_{2_n} \\ \phi_{2_{n+1}} &= \frac{1}{z}\phi_{2_n} + hR_n\phi_{1_n} \end{aligned} \tag{7}$$

and

$$\begin{aligned} \dot{\phi}_{1_n} &= A_n\phi_{1_n} + B_n\phi_{2_n} \\ \dot{\phi}_{2_n} &= C_n\phi_{1_n} + D_n\phi_{2_n}. \end{aligned} \tag{8}$$

The conservation law follows directly from these systems and there is no need to apply the techniques of the inverse scattering transform (a review of which is, for example, contained in [10]). First eliminate $\phi_{1_n}$ in (7) to obtain

$$\begin{aligned} &\left(\phi_{2_{n+2}} - \frac{1}{z}\phi_{2_{n+1}}\right)\Big/(hR_{n+1}) \\ &\quad = z\left(\phi_{2_{n+1}} - \frac{1}{z}\phi_{2_n}\right)\Big/(hR_n) + hQ_n\phi_{2_n}. \end{aligned}$$

Assuming $\phi_{2_n} = z^{-n}\alpha_n$, it follows that

$$\Delta[z^{-2n}\,\Delta\alpha_n/(hR_n)] = z^{-2n}hQ_n\alpha_n,$$

where $\Delta\alpha_n = \alpha_{n+1} - \alpha_n$. For

$$\alpha_n = \prod_{k=1}^{n} g_k,$$

one can solve recursively for the $g_n$ by assuming

$$g_n = g_n^{(0)} + g_n^{(1)}z^2 + g_n^{(2)}z^4 + \cdots. \tag{9}$$

Hence we find that

$$\begin{aligned} g_n^{(0)} &= 1 \\ g_{n+2}^{(1)} &= h^2 R_{n+1} Q_n \\ g_{n+2}^{(2)} &= h^2 R_{n+1} Q_{n-1}(1 - h^2 R_n Q_n), \qquad \text{etc.} \end{aligned} \tag{10}$$

The conservation law is obtained by eliminating $\phi_{1_n}$ from (8), using (7). This leads to

$$\dot{\phi}_{2n} = \frac{C_n}{hR_n}\left(\phi_{2_{n+1}} - \frac{1}{z}\phi_{2_n}\right) + D_n\phi_{2_n}.$$

If we again use $\phi_{2_n} = z^{-n}\alpha_n$ with $\alpha_n = \prod_{k=1}^{n} g_k$, the conservation law form of the integrable discretizations of the NLS hierarchy is obtained as

$$\frac{d}{dt}\ln g_{n+1} = \Delta\left[z^{-1}\frac{C_n}{hR_n}(g_{n+1} - 1) + D_n\right], \tag{11}$$

with the $g_k$ given by (9) and (10).

In order to obtain explicit expressions for the constants of motion pertaining to a particular equation in the NLS hierarchy, one has to substitute the appropriate choices for $C_n$ and $D_n$ in the conservation law (11). Recall (see, for example, [10]) that for the integrable discretization (3),

$$\begin{aligned} C_n &= -\frac{i}{h^2}\left[-hR_{n-1}z + hR_n\frac{1}{z}\right] \\ D_n &= \frac{i}{h^2}\left[1 - \frac{1}{z^2} + h^2 Q_{n-1}R_n\right], \end{aligned} \tag{12}$$

with $R_n = -Q_n^*$. The reduction takes the form

$$Q_n = \exp(i\omega t)\,\hat{Q}_n, \qquad R_n = \exp(-i\omega t)\,\hat{R}_n, \tag{13}$$

where $\hat{Q}_n$ and $\hat{R}_n$ are real and time independent and we choose $\omega = 1$ as before. Applied to the conservation law (11), this reduction yields

$$\Delta\left[z^{-1}\frac{C_n}{h\hat{R}_n}(g_{n+1}-1)+D_n\right]=0. \tag{14}$$

The constants of motion are given by the coefficients of the various powers of $z$. Substituting

$$g_{n+1} = 1 + h^2\hat{R}_n\hat{Q}_{n-1}z^2 + h^2\hat{R}_n\hat{Q}_{n-2}(1-h^2\hat{R}_{n-1}\hat{Q}_{n-1})\,z^4 + \cdots$$

into (14) one finds that

$$\hat{Q}_{n-1}\hat{R}_{n-1} - \hat{Q}_{n-2}\hat{R}_n(1-h^2\hat{R}_{n-1}\hat{Q}_{n-1}) = \text{const.} \tag{15}$$

It now remains to apply the reduction (13) to (3) to obtain

$$\hat{Q}_{n-2} = -\hat{Q}_n + \frac{2+h^2}{1-h^2\hat{Q}_{n-1}\hat{R}_{n-1}}\hat{Q}_{n-1}.$$

This is substituted into (15) and, if we also set $\hat{R}_n = -\hat{Q}_n$, we arrive at the required conservation law,

$$\hat{Q}_n^2\hat{Q}_{n-1}^2 + \frac{1}{h^2}[\hat{Q}_n^2 + \hat{Q}_{n-1}^2 - 2\mu\hat{Q}_n\hat{Q}_{n-1}] = E.$$

In terms of the notation used in (6) it takes the form

$$H(U,V) = \frac{1}{2}\left[U^2V^2 + \frac{1}{h^2}(U^2+V^2-2\mu UV)\right] = E. \tag{16}$$

The absence of indices means that all iterates under the integrable map (6) fall somewhere on the curve defined by (16) with the value of $E$ being determined by the initial condition $(U, V) = (U_0, V_0)$.

Here we have considered a specific choice for the coefficients in (8) pertaining to the cubic NLS equation. The same procedure applies to the other choices for the coefficients, i.e., other equations. For instance, integrable discretizations of higher order equations are obtained by applying the procedure to the other equations in the NLS hierarchy, see [12].

The expression for the homoclinic orbit (the orbit with $E = 0$ in (16)) is obtained from the one soliton solution of the integrable scheme (3), given by [10]

$$Q_n = A\sinh\tilde{w}\exp(2i\theta + \tfrac{1}{2}i(\omega+\omega^*)t) \times \operatorname{sech}(n\tilde{w} + \tfrac{1}{2}i(\omega^*-\omega)t + \xi).$$

This is of the form (13) if one chooses $\theta = 0$ which implies that $\omega$ is real (see [10], for example) and it follows that

$$\hat{Q}_n = A\sinh\tilde{w}\operatorname{sech}(n\tilde{w}+\xi).$$

It is convenient to derive the values of the contants $A$ and $\tilde{w}$ directly from (6) and we find that

$$\begin{aligned} U_n(\xi) &= \sinh w \operatorname{sech}(\tilde{w}n + \xi) \\ V_n(\xi) &= U_{n+1}(\xi), \end{aligned} \tag{17}$$

where $\mu = \cosh\tilde{w}$, $\sinh w = (1/h)\sinh\tilde{w}$, and $\xi$ is an arbitrary parameter.

Using this as a reference solution, we now proceed to study the reductions of the *nonintegrable* discretization (2) of the NLS equation.

## 3. DUFFING'S EQUATION AND KAM THEORY

Applying the reduction to the finite difference scheme (2), an analogous discretization for Duffing's equation (4) is obtained,

$$U_{n+1} - 2U_n + U_{n-1} - h^2U_n + 2h^2U_n^3 = 0. \tag{18}$$

Written as a system of first-order equations it becomes

$$\begin{aligned} U_{n+1} &= V_n \\ V_{n+1} &= -U_n + \frac{2\mu V_n}{1+h^2V_n^2} + 2h^4V_n^3\left[\frac{1/2 - V_n^2}{1+h^2V_n^2}\right]. \end{aligned} \tag{19}$$

The rather unusual form of (19) emphasizes the fact that it is viewed as a perturbation of the integrable scheme (6). The form of the perturbation is apparent from a comparison of the two equations. It is readily verified and, as it turns out, very important that this scheme is area preserving.

Analogously to the situation in Figs. 1 and 2, the solutions obtained from (6) and (19) display rather different behavior at intermediate values of $h$. The solutions of (6) are constrained by the curves (16) and therefore display no interesting irregularities, as demonstrated in Fig. 3. This figure is produced by using $h = 0.2$ and choosing different initial conditions on the $U_n$ axis. Each initial condition is allowed to evolve for many iterates under (6). Clearly all

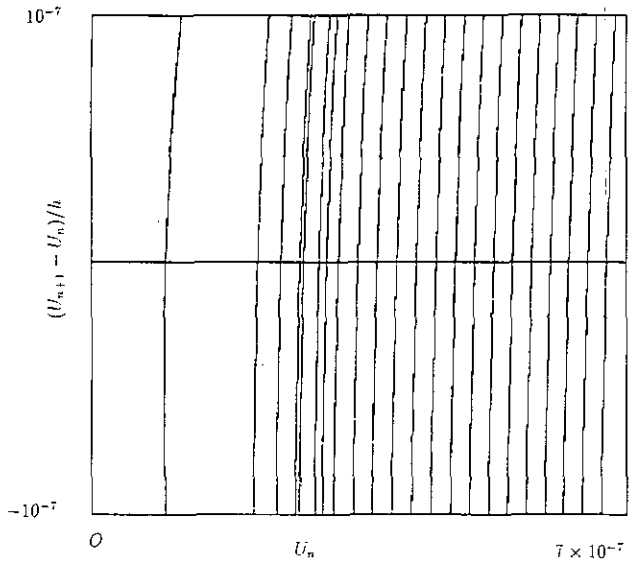


**FIG. 3.** Phase portrait obtained from the integrable discretization (6) with $h = 0.2$.

iterates fall on closed curves that are determined by (16). Solutions obtained from the nonintegrable scheme (19) are not constrained by any constant of motion and the solutions obtained from the same initial conditions used in Fig. 3 are shown in Fig. 4, again using $h = 0.2$. Note the typical features of nonintegrable symplectic mappings as one approaches the origin—invariant curves, resonant islands, and, closer to the origin, a chaotic region with islands of stability and, finally, widespread chaos. Since we are dealing with a Hamiltonian perturbation of a Hamiltonian equation, the features away from the homoclinic orbit are easily and naturally explained in terms of KAM theory. The chaos

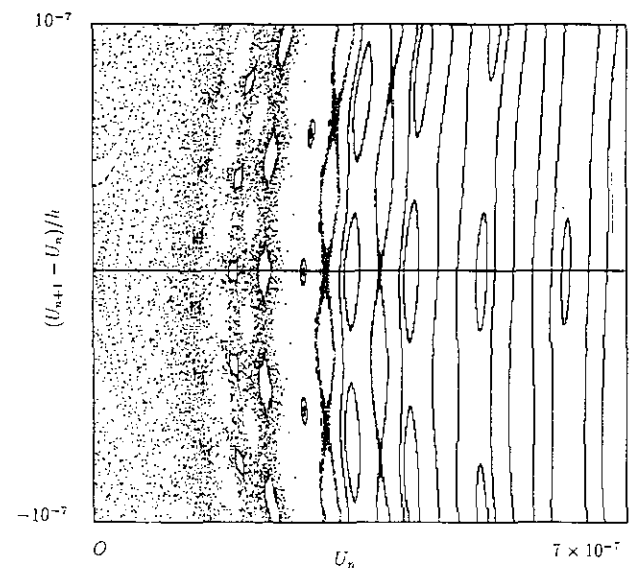


**FIG. 4.** Chaotic behavior associated with the standard discretization (19) in the vicinity of the homoclinic orbit with $h = 0.2$.

in the vicinity of the homoclinic orbit will be investigated in the next section through a Mel'nikov analysis.

Since the features shown in Fig. 4 are generic for Hamiltonian perturbations in the plane; their consequences are significant. Surrounding the resonant islands one finds separatrices (note the one shown in Fig. 4), with their own narrow bands of chaos, see, for instance, [17, 18]. In fact it is worth repeating that nonintegrable Hamiltonian perturbations of planar systems generically lead to chaotic motion in a layer surrounding a separatrix. This follows from a simple geometric argument. The key observation is that only two possibilities are consistent with area preservation in the plane. Either the perturbed system preserves all separatrices exactly, in which case the system is integrable (this is clearly a special situation) or, and this is the generic situation, the perturbed system allows homoclinic intersections and chaos. In this sense, numerical integrations of planar Hamiltonian systems using symplectic schemes are, in general, not capable of faithfully reflecting the qualitative properties of the original system. However, the chaotic regions are confined to narrow bands between the invariant KAM curves and to a region around the separatrix to the fixed point at the origin. The chaos between the invariant KAM curves shows up as a second-order effect (see, for example, [17, 18]), whereas the chaos around the separatrix at the origin is a first-order effect. A significant feature of Fig. 4 is the smallness of the chaotic region around the separatrix, relative to the value of the discretization parameter, $h$. It is therefore of considerable interest to determine the "width" of the chaotic region as a function of $h$. More specifically, we are interested to see how fast this chaotic region decreases with decreasing values of the discretization parameter. KAM theory does not provide any explanation in the vicinity of the homoclinic orbit at the origin and here we propose the use of a Mel'nikov function. This is done in the next section.

On the other hand, nonsymplectic discretizations destroy the invariant curves and, since the discrepancies are of the order of accuracy, the differences in qualitative behavior become increasingly apparent over long time integrations, as pointed out by several authors [19–22].

## 4. THE MEL'NIKOV FUNCTION

Consider a mapping

$$Q_\varepsilon: \mathbf{x} \to \mathbf{F}(\mathbf{x}) + \varepsilon \mathbf{G}(\mathbf{x}, \varepsilon), \qquad \mathbf{x} \in \mathbb{R}^2, \tag{20}$$

and $\mathbf{F}$, $\mathbf{G}: \mathbb{R}^2 \to \mathbb{R}^2$. Assume that the unperturbed map ($\varepsilon = 0$) admits a constant of motion, $H(\mathbf{x}_n) = \text{const}$, for all $n$, where $\mathbf{x}_{n+1} = \mathbf{F}(\mathbf{x}_n)$, i.e.,

$$H(\mathbf{F}(\mathbf{x}_n)) = H(\mathbf{x}_n). \tag{21}$$

Also assume that the homoclinic orbit of the unperturbed map is specified by $H(\hat{\mathbf{x}}_n(\xi))=0$, where $\xi$ is a phase factor indicating the position of the initial condition on the homoclinic orbit. For this map the splitting distance between the stable and unstable manifolds at the phase point, $\xi$, is given to first order in $\varepsilon$ by the Mel'nikov function (see, for example, [24, 13]),

$$M(\xi;\varepsilon)=\sum_{n=-\infty}^{\infty}\mathbf{G}(\hat{\mathbf{x}}_{n-1}(\xi),\varepsilon)\wedge\hat{\mathbf{v}}_n(\xi), \tag{22}$$

where $\hat{\mathbf{v}}_n(\xi)$ denotes the $n$th iterate of the tangent vector to be unperturbed homoclinic orbit from the phase point $\xi$. Also, writing the vectors in component form as $\mathbf{u}:=(u^{(1)},u^{(2)})^{\mathrm{T}}$, the wedge product is defined by $\mathbf{u}\wedge\mathbf{v}=u^{(1)}v^{(2)}-u^{(2)}v^{(1)}$. Note that $\hat{\mathbf{x}}_n(\xi)$ is evaluated at the homoclinic orbit of the unperturbed problem.

It may be useful to give another interpretation of the Mel'nikov function, apart from being a first-order estimate of the splitting distance. It is similar to the rather well-known result for continuous systems. The change in the constant of motion $H(\mathbf{x}_n)$ under the perturbed system (20) is calculated from

$$\begin{aligned}H(\mathbf{x}_{n+1})&=H(\mathbf{F}(\mathbf{x}_n)+\varepsilon\mathbf{G}(\mathbf{x}_n))\\&=H(\mathbf{F}(\mathbf{x}_n))+\varepsilon DH(\mathbf{F}(\mathbf{x}_n))\cdot\mathbf{G}(\mathbf{x}_n)+O(\varepsilon^2)\\&=H(\mathbf{x}_n)+\varepsilon DH(\mathbf{F}(\mathbf{x}_n))\cdot\mathbf{G}(\mathbf{x}_n)+O(\varepsilon^2),\end{aligned} \tag{23}$$

where we have made use of (21) and $DH$ denotes the gradient of $H$. Rewriting (23) as

$$\begin{aligned}\Delta H_n&=\varepsilon DH(\mathbf{F}(\mathbf{x}_n))\cdot\mathbf{G}(\mathbf{x}_n)+O(\varepsilon^2)\\&=\varepsilon\mathbf{G}(\hat{\mathbf{x}}_n(\xi),\varepsilon)\wedge\hat{\mathbf{v}}_{n+1}(\xi)+O(\varepsilon^2)\end{aligned} \tag{24}$$

(recall that $\mathbf{x}_{n+1}=\mathbf{F}(\mathbf{x}_n)$ on the homoclinic orbit), it follows that the Mel'nikov function is a first-order estimate of total change in the constant of motion, $H(\hat{\mathbf{x}}_n)$, over the homoclinic orbit.

In order for the first-order estimate in $\varepsilon$ of the splitting distance given by the Mel'nikov function to be valid, it is necessary for the maxima (minima) of the Mel'nikov function to be bounded away from zero as $\varepsilon\to 0$. The natural candidate for the expansion parameter in problem (19) is $h$. However, with this choice the analysis leads to a situation where the Mel'nikov function becomes exponentially small in the expansion parameter (apart from the additional complication that the unperturbed problem also depends on $h$). Here we find it convenient to consider a related map, motivated by (19),

$$\begin{aligned}U_{n+1}&=V_n\\V_{n+1}&=-U_n+\frac{2\mu V_n}{1+h^2V_n^2}+2\varepsilon h^2V_n^3\left[\frac{1/2-V_n^2}{1+h^2V_n^2}\right],\end{aligned} \tag{25}$$

avoiding these technical difficulties.

A few remarks clarifying this choice are in order. Note that the Mel'nikov function is not affected by this choice; only the interpretation of some of the results is different. By separating the expansion parameter $\varepsilon$ and the discretization parameter $h$ we ensure that $\varepsilon$ may be chosen small enough so that the Mel'nikov function provides a reliable estimate of the splitting distance for any arbitrary but fixed value of $h$. This is important when one uses the zeros of the Mel'nikov function as an indication of homoclinic intersections and chaos. In this case we anticipate needing values of $\varepsilon$ less than or equal to $O(h^2)$. For $\varepsilon$ smaller than $h^2$ the numerical method (25) is closer to the integrable one (6) than the original (19). Thus, chaos in (25) will also be an indication of chaos in (19). On the other hand, if we are interested in the behavior of the Mel'nikov function as a function of the discretization parameter $h$, the results apply equally well to the original map (19). In either case we interpret the Mel'nikov function as giving an estimate of the "width" of the chaotic layer.

In order to evaluate the Mel'nikov function we need expressions for the homoclinic orbit of the unperturbed problem and the tangent vectors to this orbit. From (16) it follows that the solution curves are parameterized by

$$\begin{aligned}\dot{U}&=\frac{\partial H}{\partial V}=U^2V+\frac{1}{h^2}(V-\mu U),\\\dot{V}&=-\frac{\partial H}{\partial U}=-UV^2-\frac{1}{h^2}(U-\mu V),\end{aligned} \tag{26}$$

which yield the tangent vectors $\hat{\mathbf{v}}_n$ needed in (22). We also require the analytical expression for the homoclinic orbit which is provided by (17). This means that we use $\hat{\mathbf{x}}_n(\xi)=(U_n(\xi),V_n(\xi))^{\mathrm{T}}$ in (22). The perturbation is obtained from a comparison of the integrable and nonintegrable schemes, (6) and (25), and is given by

$$\mathbf{G}(\hat{\mathbf{x}}_n(\xi);h)=\left(0,2h^2V_n^3\left[\frac{1/2-V_n^2}{1+h^2V_n^2}\right]\right)^{\mathrm{T}},$$

dropping the $\xi$-dependence on the right-hand side. Hence we obtain

$$\begin{aligned}M(\xi;h)=-2h^2\sum_{n=-\infty}^{\infty}U_n^3\left(\frac{1/2-U_n^2}{1+h^2U_n^2}\right)\\\times\left(U_n^2V_n+\frac{1}{h^2}(V_n-\mu U_n)\right),\end{aligned} \tag{27}$$

where $U_n$ and $V_n$ are given by (17). For future reference it is useful to rewrite the Mel'nikov function in the form

$$M(\xi; h) = h \sum_{n=-\infty}^{\infty} m(\tilde{\omega} n + \xi). \tag{28}$$

As pointed out before, simple zeros (in $\xi$) of the Mel'nikov function establishes homoclinic crossings and chaos; since chaos is generic to nonintegrable Hamiltonian perturbations, zeros of the Mel'nikov function will come as no surprise. A much more interesting question is the behavior of the Mel'nikov function as $h \to 0$. This question is easily answered whenever it is possible to evaluate the Mel'nikov sum in closed form (such as in [13]). In our case the nature of the perturbation makes this awkward. Since more complicated perturbations are envisaged, it will be expedient to develop a procedure for establishing the relevant properties without the need for a closed-form evaluation of the Mel'nikov sum.

## 5. AN EXPONENTIALLY SMALL MEL'NIKOV FUNCTION

Noting that $\tilde{w} = O(h)$, $w = O(1)$, we establish the following properties of the Mel'nikov function,

(i) $h \xrightarrow{\lim} 0$, $M(\xi; h) = 0$.

(ii) $M(\xi; h) = M(\xi + \tilde{\omega}; h)$; i.e., the Mel'nikov function is a periodic function in $\xi$ with period $\tilde{\omega}$.

(iii) $M(n\tilde{\omega}; h) = 0$ for all integers $n$.

An outline of a proof is as follows:

(i) A Taylor expansion shows that

$$\mathbf{G}_{n-1}(\xi) \wedge \mathbf{v}_n(\xi) = -2hU_n^3(\tfrac{1}{2} - U_n^2)\, U_n' + O(h^2),$$

where a prime denotes a derivative with respect to the argument (note the slight change in notation). Substituting the theoretical solution of the homoclinic orbit yields

$$\mathbf{G}_{n-1}(\xi) \wedge \mathbf{v}_n(\xi) \to 2h \operatorname{sech}^4 A_n(\xi)[\tfrac{1}{2} - \operatorname{sech}^2 A_n(\xi)] \times \tanh A_n(\xi), \tag{29}$$

where $A_n(\xi) = hn - \xi$. Using $A_n(\xi) \to A(\zeta; \xi) := \zeta - \xi$, the sum converts to an integral in $\zeta$ as $h \to 0$ and, since the integrand is odd, the integral is zero.

(ii) This follows directly from (28), taking into account the freedom provided by summation in $n$.

(iii) One can verify directly from (27) that $M(0; h) = 0$; the periodicity takes care of the remaining zeros.

Hence we have established that the homoclinic orbit is restored in the limit $h \to 0$, i.e., as the numerical method converges to the analytic solution. Also, the existence of simple zeros shows the presence of chaos, as expected from an area-preserving map. Although not too surprising in itself, these results enable us to investigate the behavior of the Mel'nikov function at small but finite values of $h$. In fact, we now proceed to show that the Mel'nikov function is exponentially small as a function of $h$.

The Fourier coefficients of the Mel'nikov function are given by

$$\hat{M}_n(h) = \frac{1}{\tilde{\omega}} \int_0^{\tilde{\omega}} M(\xi; h) \exp(-i\mu_n \xi)\, d\xi,$$

where $\mu_n = 2\pi n/\tilde{\omega}$. Making use of (28), interchanging summation and integration (allowed because of the uniform convergence in $\xi$ for finite values of $h$), one finds that

$$\hat{M}_n(h) = \frac{h}{\tilde{\omega}} \int_{-\infty}^{\infty} m(z) \exp(-i\mu_n z)\, dz. \tag{30}$$

It is well known (see, for example, [25]) that the leading order behavior of this integral is determined by the singularities of $m(z)$ in the complex plane. More specifically, the rate of decay of $\hat{M}_n(h)$, as a function of $h$, is determined by the distance of the nearest poles of $m(z)$ to the real axis. Since we find poles at $z = \pm i\pi/2$ and $\pm h \pm i\pi/2$, it follows that the leading order behavior is given by

$$\hat{M}_n(h) \sim \exp(-\pi^2 n/\tilde{\omega}). \tag{31}$$

Since $\tilde{\omega} = O(h)$ we find that all Fourier modes, $n \neq 0$, decay at least at the exponential rate of $\pi^2/h$. It remains to establish the exponential decay of $\hat{M}_0$. We outline the geometrical argument leading to this result. Take the region in phase space formed by following the stable and unstable manifolds from the fixed point to their first intersection. If this region is mapped under one application of the map, part of it, an area of phase space bounded between the stable and unstable manifolds, leaves the region. For an area-preserving map this loss in area is compensated for the same area entering the region from outside. Thus one establishes that the areas of the regions bounded between the stable and unstable manifolds are the same and it follows that the average splitting distance, or $\hat{M}_0$, is zero. Hence, we have demonstrated that the Mel'nikov function decays faster than any polynomial power of $h$.

The property (31) is a central result of this study and implies that the "chaotic layer" around the homoclinic orbit at the origin decreases at an exponential rate for the discretization (25). A more detailed discussion of how it relates to the original discretization (19) is given in the concluding

section. A careful study of our arguments leading to the exponential decay reveals that it depends on three general properties, namely, the periodicity and analyticity of the Mel'nikov function and the area-preserving property of the map. The periodicity is a direct consequence of the general construction of the Mel'nikov function, involving a natural arbitrary phase $\xi$. The discretization parameter provides the period of $O(h) - U_n$ is an approximation of $u(nh)$. The analyticity derives from the smoothness of the homoclinic orbit and the perturbation, as well as the fact that it approaches the hyperbolic fixed point at an exponential rate. More specifically, the distance of the poles to the real axis in the expression for the homoclinic orbit and the perturbation determines the rate of decay of the Mel'nikov function. Clearly it is important that the mean term $\hat{M}_0$ vanish as it does for area-preserving maps. If we are not dealing with symplectic maps; $\Delta H$ in (24) need not even change sign, in which case $\hat{M}_0$ is clearly nonzero. In fact, it is of the order of the accuracy of the scheme; i.e., it is algebraic.

It is reasonable to expect these conditions to apply quite generally for symplectic discretizations of one degree of freedom Hamiltonian maps. The conclusions of our investigation are therefore not confined to the particular problem discussed in this study.

Since one may evaluate the Mel'nikov sum in closed form

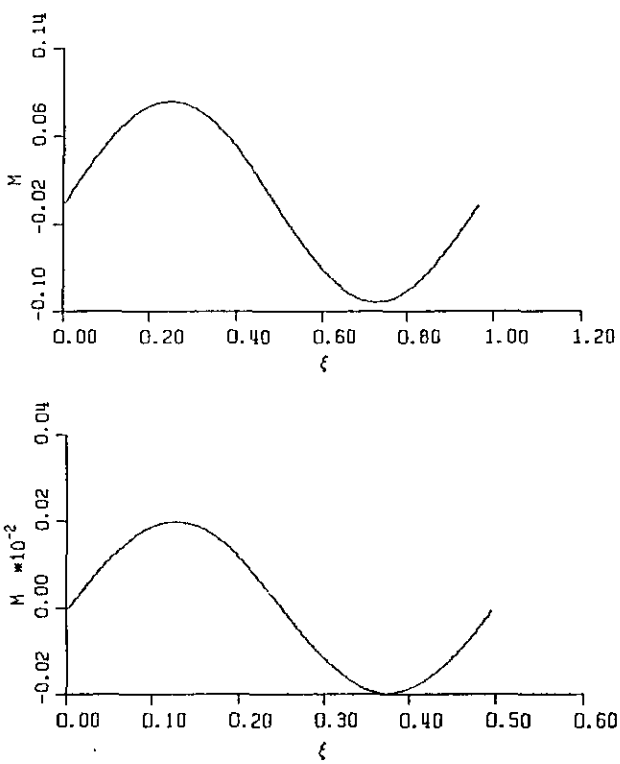


**FIG. 5.** The Mel'nikov function as a function of the reference point, $\xi$: (a) $h = 1$; (b) $h = 0.5$.

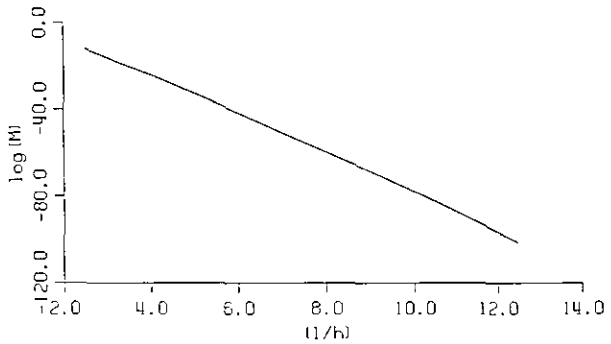


**FIG. 6.** Exponential decay in the maximum value of the Mel'nikov function for decreasing $h$.

for certain linear perturbations [13], it is possible to directly verify our conclusions for these specific examples. It turns out that their Mel'nikov function indeed decays exponentially in $h$, with rate of decay $\pi^2/h$ as predicted by an asymptotic pole analysis of the relevant integrals.

We conclude this section with a numerical verification of our analytical results. Figure 5 shows $M(\xi; h)$ as a function over one period of $\xi$ for $h = 1$ and $h = 0.5$. One clearly observes the rapid decay of the Mel'nikov function with decreasing values of $h$. Evidence of exponential decay is provided in Fig. 6. It shows the logarithm of the maximum value of the Mel'nikov function as a funcion of $1/h$. The rate of decay is determined numerically as $M \propto \exp(-9.4/h)$, at $h = 0.1$ (in general agreement with our asymptotic estimates). These calculations have been done in Mathematica, using 55 digits precision!

## 6. SYMPLECTIC SCHEMES

The finite difference scheme (19) is an area-preserving scheme and therefore preserves the symplectic character of one degree of freedom Hamiltonian systems. Although this scheme does not readily extend to higher dimensional systems, a large number of symplectic schemes that can be applied to higher dimensional Hamiltonian systems have been derived; see, for instance, [19–23]. Here we choose to compare the second- and fourth order symplectic schemes of Forest and Ruth [14] with the finite difference scheme (19). For a separable Hamiltonian,

$$H(q, p) = A(p) + V(q), \tag{32}$$

their schemes are written in the general form,

$$\begin{aligned} p_{i+1} &= p_i - C_i h \frac{d}{dq} V(q), \\ q_{i+1} &= q_i + D_i h \frac{d}{dp} A(p), \end{aligned} \tag{33}$$

where $i = 1, ..., N$ and the coefficients $C_i$'s and $D_i$'s are determined in order to render the scheme symplectic and of $O(h^N)$. Here $p_1$, $q_1$ are the numerical approximations at time $t$ and $p_{N+1}$, $q_{N+1}$ are the approximations at $t + h$. For the second-order scheme ($N = 2$), it follows that [14]

$$C_1 = 0, \qquad C_2 = 1, \qquad D_1 = \tfrac{1}{2} = D_2. \tag{34}$$

In our example,

$$A(p) = \tfrac{1}{2}p^2, \qquad V(q) = \tfrac{1}{2}(-u^2 + u^4).$$

Again choosing $h = 0.2$ and using exactly the same initial conditions as in Fig. 4, we obtain the phase portrait shown in Fig. 7. A comparison with Fig. 4 shows that the two schemes share the same qualitative features. This is not surprising in view of our arguments about the genericity of our results.

We attached special significance to the fact that the Mel'nikov function decreases exponentially with decreasing $h$. This shows that the qualitative features (homoclinic orbit) of the problem are recovered faster than the order of the discretization, possibly exponentially fast; see the discussion in the last section. This suggests that higher order symplectic schemes may not be able to perform significantly better than the low order schemes, at least as far as qualitative features are concerned. For this reason it is of interest to investigate the behavior of a higher order symplectic scheme. The fourth-order ($N = 4$) Forest and Ruth scheme uses

$$\begin{aligned} &C_1 = 0, \qquad C_2 = 2s + 1, \\ &C_3 = -4s - 1, \qquad C_4 = C_2, \\ &D_1 = s + \tfrac{1}{2}, \qquad D_2 = -s = D_3, \qquad D_4 = D_1, \end{aligned} \tag{35}$$

where $s = \frac{1}{6}(2^{1/3} + 2^{-1/3} - 1)$.

The phase portrait using $h = 0.2$ and the same scaling as in Figs. 4 and 7 is shown in Fig. 8. Although the details differ, the fourth-order scheme has the same qualitative features as the two second-order schemes. In particular, the region of widespread chaos has *not* been reduced. This is consistent with an exponentially small (in $h$) splitting distance.

Because of the current interest in the construction of symplectic discretizations of Hamiltonian systems, it may be instructive to summarize the main differences between symplectic and nonsymplectic discretizations forthcoming from this study.

We have pointed out that nonintegrable symplectic discretizations invariably lead to chaotic numerical solutions.

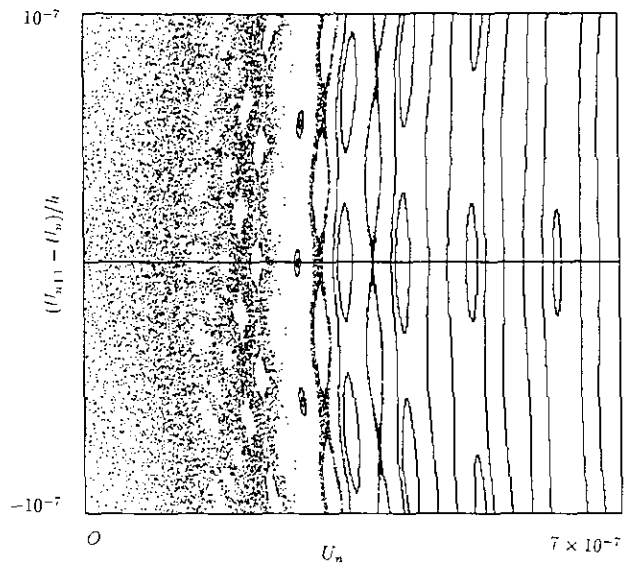


FIG. 7. The phase portrait for the second order symplectic scheme (34), $h = 0.2$.

For small values of the discretization parameter the chaos is observed in a region surrounding the separatrix of the original system and, second, also in regions between the invariant KAM curves. Our Mel'nikov analysis of this region indicates a rapid (exponential) decrease of the size of this chaotic region, much faster than the order of accuracy of the discretization. For sufficiently small perturbations, i.e., sufficiently small $h$, the invariant KAM curves divide two-dimensional phase space into disconnected invariant regions and the chaos away from the separatrix is confined to these narrow regions. It is only observed under substan-

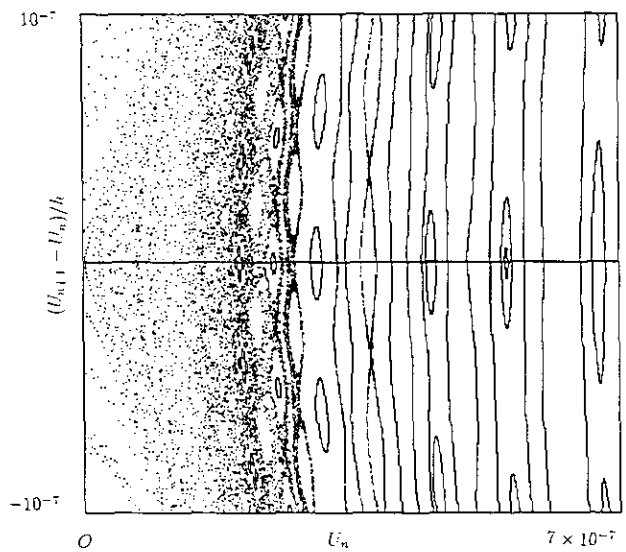


FIG. 8. The phase portrait for the fourth order symplectic scheme (35), $h = 0.2$.

tial magnification and is easily overlooked. In any event, the qualitative situation improves rapidly as $h \to 0$.

Our analysis does not allow the same desirable properties for nonsymplectic discretizations. In the first place, it destroys the KAM curves, allowing the solution to wander around in phase space. In the second place, the average splitting distance is nonzero. Although the chaos may disappear at an exponential rate the nonzero mean ($\hat{M}_0$ in (30)) will in general decrease at the order of the discretization and not necessarily faster. Consequently explicit Runge–Kutta [23] methods for example, are not generally desirable.

## 7. CONCLUSIONS

One has to be careful about the interpretation of the exponential decay of the Mel'nikov function for the scheme (19). The Mel'nikov function is a first-order approximation of the splitting distance—the true indicator of chaos. If the Mel'nikov function becomes exponentially small in the expansion parameter, it is strictly necessary to take higher order terms in the asymptotic expansion for the splitting distance into account. In fact, in order to "rigorously" show that the splitting distance becomes exponentially small, it is necessary to show that all terms in its perturbation expansion become exponentially small (though the leading order analysis is rather general and subsequent terms depend on the first term.) This is a more sophisticated problem and one we hope to pursue elsewhere. Nevertheless, by showing that the Mel'nikov function decreases exponentially, we have given very strong indications that the qualitative behavior is recovered faster than the order of the discretization. Hence even though there are numerical indications that the actual rate of decrease of the splitting distance may be exponential, this has not been established rigorously. It is also important to note that it is the *qualitative* behavior that is recovered rapidly. The numerical orbit remains an approximation of the analytical orbit. The order of this approximation is determined by the order of the discretization, as usual. The situation for higher dimensional integrable Hamiltonian systems remains to be studied.

Our analysis draws a sharp distinction between symplectic and nonsymplectic methods in the plane. For nonsymplectic methods (e.g., explicit Runge–Kutta) there is no reason to expect that the homoclinic orbit will be restored at a rate any faster than the order of the discretization. This work provides further theoretical justification for the use of symplectic schemes for solving integrable Hamiltonian systems.

We hope to return to some of these issues in future work and also extend it to problems with more degrees of freedom.

## ACKNOWLEDGMENTS

This work (MJA) is partially supported by the NSF Grants No. DMS-8916182, the Office of Naval Research Grant No. N00014-90/J/2/8 and the Air Force Office of Scientific Research Grant No. AFOSR-90-0039. We are grateful to R. W. Easton, J. Meiss, and H. Segur for valuable discussions.

## REFERENCES

1. E. A. Overman II, D. W. McLaughlin, and A. R. Bishop, Coherence and chaos in the driven damped sine–Gordon equation: measurement of the soliton spectrum, *Physica D* **19**, 1 (1986).
2. A. R. Bishop, D. W. McLaughlin, M. G. Forest, and E. A. Overman II, *Quasi-periodic route to chaos in a near-integrable PDE: Homoclinic* crossings, *Phys. Lett. A* **127**, 335 (1988).
3. N. Ercolani, M. G. Forest, and D. W. McLaughlin, Geometry of the modulational instability. Part III. Homoclinic orbits for the periodic sine–Gordon equation, *Physica D* **43**, 349 (1990).
4. N. Ercolani, D. W. McLaughlin, and M. G. Forest, Notes on Mel'nikov integrals for models of the driven pendulum chain, preprint, 1989.
5. N. N. Akhmedieva, V. M. Eleonskii, and N. E. Kulagin, Generation of periodic trains of picosecond pulses in an optical fiber: Exact solutions, *Sov. Phys. JETP* **62**, 894 (1985).
6. B. M. Herbst and M. J. Ablowitz, Numerically induced chaos in the nonlinear Schrödinger equation, *Phys. Rev. Lett.* **62**, 2065 (1989).
7. B. M. Herbst and M. J. Ablowitz, "On Numerical Chaos in the Nonlinear Schrödinger Equation," *Integrable Systems and Applications*, edited by M. Balabane, P. Lochak, and C. Sulem, Lecture Notes in Physics, Vol. 342 (Springer-Verlag, Berlin, 1989).
8. M. J. Ablowitz and B. M. Herbst, On homoclinic structure and numerically induced chaos for the nonlinear Schrödinger equation, *SIAM J. Appl. Math.* **50**, 339 (1990).
9. M. J. Ablowitz and B. M. Herbst, "On Homoclinic Boundaries in the Nonlinear Schrödinger Equation," in *Hamiltonian Systems, Transformation Groups and Spectral Transform Methods*, edited by J. Harnad and J. E. Marsden (CRM Montreal, 1990).
10. M. J. Ablowitz and H. Segur, *Solitons and the Inverse Scattering Transform* (SIAM, Philadelphia, 1981).
11. D. W. McLaughlin and C. M. Schober, Chaotic and homoclinic behavior for numerical discretizations of the nonlinear Schrödinger equation, preprint, 1990.
12. E. E. Ryan, Ph. D. thesis, Clarkson University, 1991 (unpublished).
13. M. L. Glasser, V. G. Papageorgiou, and T. C. Bountis, Mel'nikov's function for two-dimensional mappings, *SIAM J. Appl. Math.* **49**, 692 (1989).
14. E. Forest and R. D. Ruth, Fourth-order symplectic integration, *Physica D* **43**, 105 (1990).
15. E. M. McMillan, "A Problem in the Stability of Periodic Systems," in *Topics in Modern Physics—A Tribute to Edward U. Condon* (Colorado Asso. Univ. Press, Boulder, CO, 1971, p. 219.)
16. M. J. Ablowitz and J. F. Ladik, *Stud. Appl. Math.* **55**, 213 (1976).
17. A. J. Lichtenberg and M. A. Lieberman, *Regular and Stochastic Motion* (Springer-Verlag, New York, 1983).
18. J. Guckenheimer and P. Holmes, Nonlinear oscillations, dynamical systems, and bifurcations of vector fields (Springer-Verlag, New York, 1983).
19. F. Kang, Difference schemes for Hamiltonian formalism and symplectic geometry, *J. Comput. Math.* **4**, 279 (1986).

20. F. Kang and M.-Z. Qin, "The Symplectic Methods for the Computation of Hamiltonian Equations," *Numerical Methods for Partial Differential Equations*, edited by Y.-I. Zhu and B.-Y. Guo, Lecture Notes in Mathematics, Vol. 1297 (Springer-Verlag, New York/Berlin, 1987).
21. C. Scovel, "Symplectic Numerical Integration of Hamiltonian Systems," in *Proceedings, MSRI Workshop on Geometry of Hamiltonian Systems, 1990*, to appear.
22. P. J. Channel and C. Scovel, Symplectic integration of Hamiltonian systems, *Nonlinearity* **3**, 231 (1990).
23. J. M. Sanz-Serna, Runge–Kutta schemes for Hamiltonian systems, *BIT* **28**, 877 (1988).
24. R. W. Easton, Computing the dependence on a parameter of a family of unstable manifolds: Generalized Mel'nikov formulas, *Nonlinear Anal. Theory, Methods Appl.* **8**, 1 (1984).
25. J. D. Murray, *Asymptotic Analysis* (Springer-Verlag, New York, 1984).